THE ISO-LWS SPECTRUM OF T TAURI

L. Spinoglio[1], T. Giannini[1,2,5], P. Saraceno[1], A.M. Di Giorgio[1], B. Nisini[1], S. Pezzuto[1], F. Palla[3], C. Ceccarelli[4], D. Lorenzetti[5], H.A. Smith[6] & G.J. White[7]

[1]Istituto di Fisica dello Spazio Interplanetario, CNR, Roma, Italy.
[2]Università La Sapienza, Roma, Italy.
[3]Osservatorio Astrofisico di Arcetri, Firenze, Italy.
[4]Laboratoire d'Astrophysique de l'Observatoire de Grenoble, Grenoble, France.
[5]Osservatorio Astronomico di Roma, Monte Porzio, Italy
[6]Smithsonian Center for Astrophysics, Cambridge, US.
[7]Physics Department, Queen Mary & Westfield College, University of London, London, UK.

ABSTRACT

With the LWS spectrometer on-board the Infrared Space Observatory (ISO), we have detected toward T Tauri strong emission from high-J (J>14) CO, H_2O and OH transitions over the wavelength range from 40 to 190 μm. In addition, the LWS spectrum shows the [OI]63 μm and 145 μm and [CII]158 μm atomic lines. The molecular emission can be explained by a single emission region at T$\sim$300-900 K and n_{H_2} $\sim 10^{5-6}$cm^{-3}, with a diameter of about 2-3 arcsec, corresponding to 300-400 AU (at the distance of 140 pc). We derive a water abundance of 1-3 $\cdot 10^{-5}$ and an OH abundance of $\sim 3 \cdot 10^{-5}$ with respect to molecular hydrogen, implying H_2O and OH enhancements by more than 10 with respect to the ambient gas abundance.

Key words: Stars: Circumstellar matter; Stars: Pre-main Sequence (T Tauri); Infrared: spectroscopy; molecular emission.

1. INTRODUCTION

T Tauri is at the same time the prototype of a class of pre-main sequence stars (the T Tauri's) and a very peculiar object. It is in fact a binary system (Dyck et al. 1982, Ghez et al. 1991), consisting of T Tauri N, which is optically visible, and T Tauri S, visible in the infrared, at an angular distance of 0.7 arcsec, corresponding to 100 AU at the 140 pc distance of the Taurus Auriga dark cloud.

T Tauri has one of the highest luminosities at millimeter wavelengths among pre-main sequence stars, and it is therefore associated to a substantial amount of mass of dust (Adams et al. 1990, Beckwith et al. 1990). A circumstellar disk has been detected both with CO interferometry and infrared scattered light (Weintraub et al. 1989, Momose et al. 1996). Later, millimeter continuum interferometry at 0.9 and 3mm (Hogerheijde et al. 1997, Akeson et al 1998, respectively) was used to associate the circumstellar disk around T Tauri N. Molecular emission shows a complex outflow system (e.g. Schuster et al. 1997 and references therein) that could be originated from the different components of the binary system. The presence of fast stellar winds are observed through forbidden optical line emission (Bohm & Solf 1994).

Strong and extended H_2 rotovibrational emission was find quite early around T Tauri (Beckwith et al. 1990). Recently, high resolution H_2 imaging (Herbst et al. 1996, Herbst et al. 1997) indicated that the interaction of two outflow systems with the ambient molecular cloud can explain the complex molecular hydrogen morphology of T Tau.

2. OBSERVATIONS

T Tauri (RA(1950) = 4^h 19^m $4^s.1$, Dec(1950) = $+19^o$ $25'$ $5''$) has been observed with ISO (Infrared Space Observatory) using the LWS (Long Wavelength Spectrometer, Clegg et al. 1996). A full low resolution (R $\sim$ 200) spectrum of the source from 45 to 197 μm has been obtained during revolution 680. The beamsize is on average 80 arcsec, depending on the wavelength. The spectrum was collected in 23 full grating scans oversampled at 1/4 of a resolution element and each spectral sample was integrated for a total of 11.5 sec, for a total integration time of 4265 sec. The raw data have been reduced and calibrated by using the version 7 of the LWS pipeline with an absolute accuracy of about 30 % (Swinyard et al. 1996). Post-pipeline processing has been performed with the ISAP (ISO Spectral Analysis Package) package and included removal of spurious signals due to cosmic ray impacts and averaging the grating scans of each detector.

Proceedings of the Conference "The Universe as seen by ISO", Paris, France, 20–23 October 1998 (ESA SP-427, March 1999)

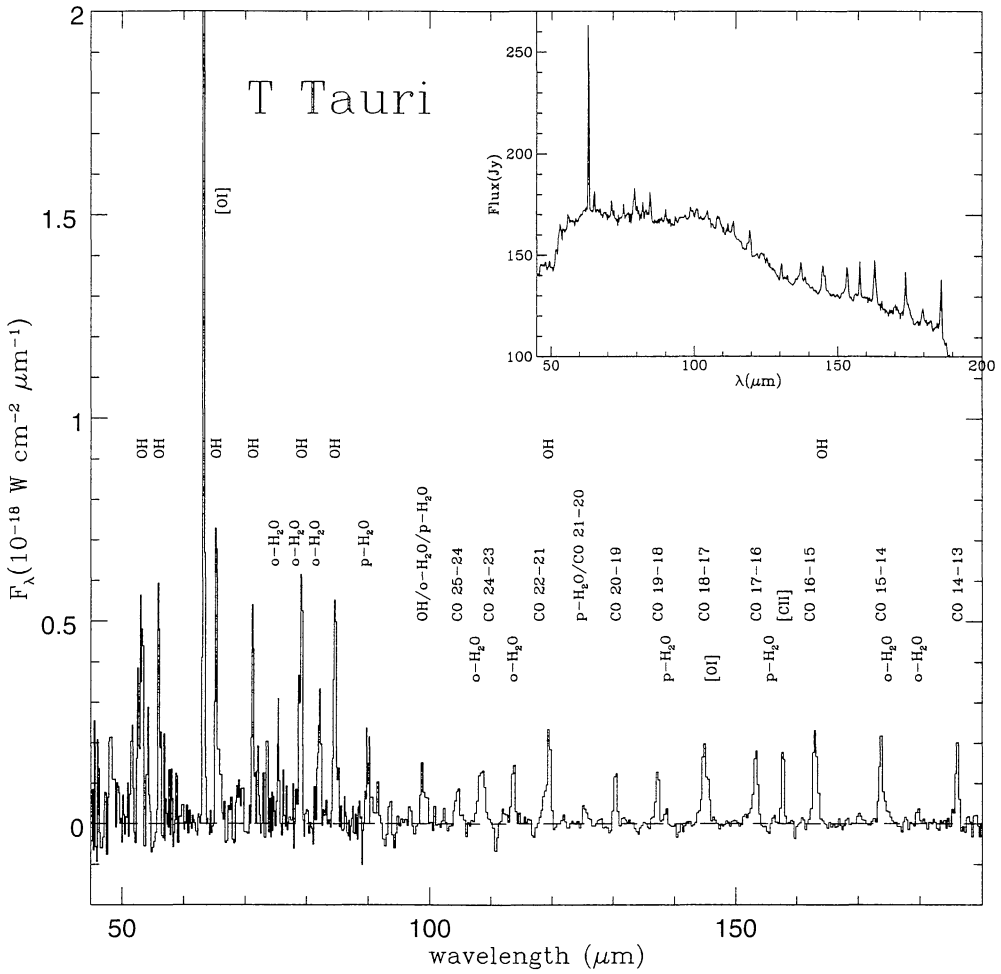

Figure 1. The LWS spectrum, from which the continuum emission has been subtracted, with the identification of the detected lines. The upper-right panel presents the observed spectrum.

3. THE EMISSION LINE SPECTRUM

The far-infrared spectrum of T Tauri is very rich of molecular emission lines from the rotational spectra of carbon monoxide, water and OH. A thorough analysis and interpretation of the complete spectrum will be presented in a forthcoming paper (Spinoglio et al. 1998), while we outline here the preliminary modeling.

All the CO transitions with J_{up} = 14-25 appear in the spectrum, except the line with J_{up}=23. Water lines are observed both in the ortho and para form. Most of the back-bone lines up to excitation temperatures of about 650 K are detected for the ortho-water and up to nearly 400 K for the para-water, plus most of the strongest transitions falling in the LWS spectral range. In addition to CO and water, also the OH lines are detected and are particularly strong, with excitation temperatures up to 600 K. [OI] 63 μm and 145 μm and [CII] 158 μm are the only atomic lines present in the spectrum.

A large velocity gradient (LVG) code, solving the level population equations in a plane parallel geometry (Nisini et al. 1998, Nisini et al. 1999, Giannini et al. 1998) has been used to model the observed molecular emission line intensities from CO, H_2O and OH. As a first approximation, for the CO and H_2O models, the local radiation field has not been taken into account in the radiation transfer calculations, while for the OH we also considered models that included the infrared local radiation field.

As can be seen in Nisini et al. (1998), the model free-parameters are many (gas temperature and density, intrinsic width of the line, column density and emitting area or filling factor, which is related to both number and column densities) and cannot easily be constrained simultaneously. Given the assumption that all the molecular lines originate from the same emitting gas, we started our analysis by deriving the range of temperature and density that is allowed from fitting the CO lines, that are likely to be optically thin. Then we used the range found from the CO to model the water and OH lines, which, in contrast with the CO lines, have high optical depths having their low lying energy levels connected by strong radiative transitions in the far-infrared.

4. CO EMISSION

For the CO model, we computed the collisional downward rates for levels with $J_{up} < 60$ and T > 100 K using the γ_{J0} coefficients taken from McKee et al. (1982), while the upward rates were computed using the principle of detailed balance. Radiative decay rates were taken from Chackerian & Tipping 1983. The distribution of the observed CO line fluxes as a function of the rotational quantum number (Fig.2) shows that the transitions with J_{up} =24 and 25 have a flux level too high to be explained by the same gas component of the other lines and they may indicate the presence of a warmer gas emission. We have therefore considered for our fit only the transitions with J_{up} lower than 22. An estimate of the intrinsic linewidth dV can be given if we relate the observed emission with the outflow/wind activity taking place in the close environment of the T Tauri binary system. The molecular outflow has been traced by different lines in the near infrared and millimeter wavelengths (H_2, CO, HCO^+), showing linewidths of a few km s^{-1}. Assuming in the models a line-width of 10 kms^{-1}, our data are consistent with gas temperatures ranging from T =300 to 900 K and molecular hydrogen densities of n = $10^{5-6} cm^{-3}$. The two "best fit" models found have:

T = 300 K and n_H=$4 \cdot 10^6 cm^{-3}$;

T = 900 K and n_H=$2 \cdot 10^5 cm^{-3}$.

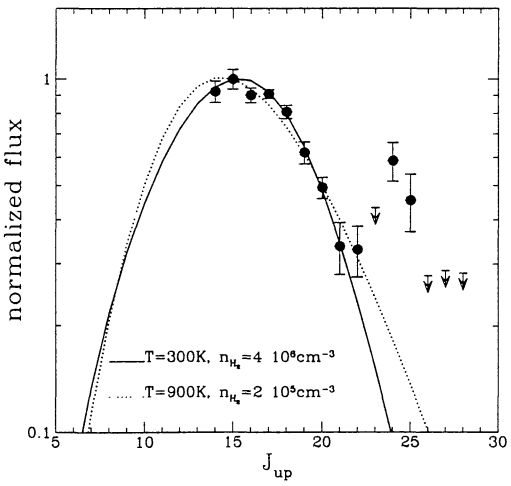

Figure 2. Model fits through the observed CO lines. The range of temperatures and densities compatible with the observations are indicated. The higher observed J lines (J=24,25 and 26) have fluxes too high to be fitted by the same parameters as the other lines, suggesting the presence of a second component.

5. H_2O EMISSION

As outlined in the previous section, we adopted the temperature and density as derived from the CO lines modeling to fit the observed H_2O line fluxes.

We considered in the computation 45 levels for both the ortho and para species (i.e., excitation energies up to $\sim$ 2000 K): radiative rates are taken from Chandra et al. (1984) while the H_2O-H_2 collision rates are derived from Green et al. (1993). We assumed an ortho/para abundance ratio of 3, equal to the ratio of the statistical weights of their nuclear spins.

Besides temperature and density, which are already determined from the CO model, the water line intensities depend on the velocity gradient in the region (dV/dr) and on the projected area of the emission region. The optical depth in the lines is directly proportional to the velocity gradient and inversely proportional to the water density, i.e. it is proportional to the quantity dV/N(H_2O), where N(H_2O) is the water column density. Since the ratios of different lines depend on their relative optical depths, we can use them to constrain the dV/N(H_2O) value. On the other hand, the absolute line intensity depends on both column density and projected area of the emission region, and therefore if we assume a velocity linewidth dV, we can estimate both the column density and the emission region size.

The two models that best represent the observed CO data, with T=300 K and T=900 K, respectively, have dV/N(H_2O) = $5 \cdot 10^{-17}$ km s^{-1} cm^2 and $7 \cdot 10^{-17}$ km s^{-1} cm^2.

Adopting a velocity of 10 km s^{-1}, we derive a water column density of (1.4-2)10^{17} cm^{-2}, while the projected area results to be of (4-9) $arcsec^2$ (*i.e.* 300-400 AU of diameter assuming spherical symmetry), implying that only about 3% of the emission is filling the LWS beam.

Using this emission area, the CO column density that we derive from the observed CO absolute line fluxes is N(CO) = (1.5)10^{18} cm^{-3} and therefore a H_2O/CO abundance ratio of X(H_2O)/X(CO)$\sim$0.1-0.3. Assuming a standard CO abundance of 10^{-4}, the water abundance with respect to H_2 is $\sim$ 1-3$\cdot 10^{-5}$. This value implies an enhancement with respect to the ambient gas of at least a factor of 10.

High H_2O abundances are fairly common in young stellar objects: the ISO spectrometers have in fact found strong emission from gas-phase H_2O from massive young stars (Helmich et al. 1996, van Dishoeck & Helmich 1996) and from low mass outflow driving sources (Liseau et al. 1996, Saraceno et al. 1998, Ceccarelli et al. 1998, Nisini et al. 1998) with abundances in the range 1-5$\cdot 10^{-5}$, with the exception of L1448mm (Nisini et al. 1999) and Orion (Harwit et al. 1998), whose H_2O lines indicate a water abundance as high as $\sim$ $5 \cdot 10^{-4}$.

6. OH EMISSION

For the OH models, we have considered 20 levels. The collisional downward rates are from Offer & van Dishoeck 1992 and the radiative decay rates are from the HITRAN catalogue (Rothman et al. 1987).

If we adopt the same parameters as derived from the above analysis also for the OH, we find that a better agreement between data and models is achieved with the lower temperature model (T = 300 K). We can estimate from this latter a N(OH) column density of $\sim 4 \cdot 10^{17}$ cm^{-3} and therefore a X(OH)/X(H_2) $\sim 2.7 \cdot 10^{-5}$, i.e. twice the water abundance. Because T Tauri is relatively bright in the continuum at the far infrared wavelengths (see Fig.1), we also computed models for the OH transitions including the field originated from dust at a temperature of 300K. The low-lying transitions of OH are in fact easily radiatively pumped by a local field. We found that the inclusion of the local infrared radiation field increases the emission in the lines with λ less than 100 μm.

Table 1 summarizes the physical quantities derived from the observed molecular spectra of CO, H_2O and OH, adopting the two models considered: the column densities and the total cooling luminosities are given for each molecular species.

Table 1. Physical parameters of the molecular emission

	"lower T"	"higher T"
Gas temperature T (K)	300	900
Gas density $n_{H_2}(cm^{-3})$	$4{\cdot}10^6$	$2{\cdot}10^5$
N_{CO} (cm^{-2})	$2.4 \cdot 10^{18}$	$7 \cdot 10^{17}$
N_{H_2O} (cm^{-2})	$2 \cdot 10^{17}$	$1.4 \cdot 10^{17}$
N_{OH} (cm^{-2})	$4{\cdot}10^{17}$	$4 \cdot 10^{17}$
L_{CO} ($L_\odot$)	0.0096	0.010
L_{H_2O} ($L_\odot$)	0.014	0.009
L_{OH} ($L_\odot$)	0.019	0.009

We speculate that the presence of the stellar radiation field (see, e.g., Herbig & Goodrich 1986) may dissociate the water in favour of OH. In Herbig AeBe stars this situation is even more extreme and the far-infrared spectra do not show any sign of water emission (Giannini et al. 1998)

7. ATOMIC EMISSION

The neutral oxygen lines and the ionized carbon line fluxes are consistent with photodissociation region models (Kaufman et al. 1999) with high density gas (log n = 5.5cm^{-3}) illuminated from a weak continuum (log G_o = 2.5, where G_o is the incident far-ultraviolet flux in units of 1.6×10^{-3}erg cm^{-2}s^{-1}, Habing 1968). We note that the same values of the density are derived from the molecular lines.

Finally the ratio of [OI] 63μm/145μm=28.3 is such that no oxygen self-absorption is needed, indicating that probably no colder gas is located in front of the source, as expected from the geometry of the outflow system (in the direction of the observer), that could have swept out the gas.

REFERENCES

Adams, F.C., et al. 1990, ApJ, 357, 606.

Akeson, R.L., Koerner, D.W., Jensen, E.L.N. 1998, ApJ, 505, 358.

Beckwith, S.V.W., et al. 1990, AJ, 99, 924.

Bohm, K.-H., Solf, J. 1994 ApJ, 430, 277.

Ceccarelli C., et al. 1998, A&A, 331, L17.

Chackerian C. & Tipping R.H. 1983, J. of Molecular Spectroscopy, 99,431

Chandra S., Varshalovich D.A. & Kegel W.H. 1984, A.A.S.S., 55, 51.

Clegg P.E., et al., 1996, A&A 315, L38

Dyck, H. M., Simon, T., Zuckerman, B. 1982, ApJ, 255, 103.

Ghez, A.M., et al 1991, AJ, 102, 2066.

Giannini T., et al. A&A, 1998, submitted.

Green S., Maluendes S., McLean A.D. 1993, ApJ, 85.181

Habing, H.J., 1968, Bull.Astr.Inst.Netherlands, 19, 421.

Harwit et al. 1998, ApJ, 497, L105.

Helmich, F.P., et al. 1996, A&A 315, L173.

Herbig, G.H. & Goodrich, R.W. 1986, ApJ, 309, 294.

Herbst, T.M. et al. 1996, AJ, 111, 2403.

Herbst, T.M., Robberto, M, and Beckwith, S.V.W., 1997, AJ, 114, 774.

Hogerheijde, M.R., et al. 1997, ApJ, 490, L99.

Kaufman, M. et al., 1999, ApJ, submitted.

Liseau R., et al. 1996, A&A 315, L181.

McKee, C.F. et al. 1982 ApJ, 259, 647.

Momose, M. et al. 1996, ApJ, 470, 1001.

Nisini B., et al. 1999, A&A, submitted.

Nisini B., et al. 1998, A&A, in press.

Offer, A.R. & van Dishoeck, E.F. 1992, MNRAS, 257, 377.

Rothman, L.S., et al. 1987, Appl.Opt., 26, 4078.

Schuster, K.-F., Harris, A.I., Russell, A.P.G, 1997, A&A, 321, 568.

Saraceno, P., et al. 1998, in preparation.

Spinoglio, L., et al. 1998, in preparation.

Swinyard, B.M., et al. 1996, A&A, 315, L43.

van Dishoeck,E.F., & Helmich, F.P. 1996, A&A 315, L177

Weintraub, D.A., et al. 1989, ApJ, 344, 915.